



# Room-temperature multiferroic behavior in layer-structured Aurivillius phase ceramics

Cite as: Appl. Phys. Lett. **117**, 052903 (2020); <https://doi.org/10.1063/5.0017781>

Submitted: 09 June 2020 . Accepted: 25 July 2020 . Published Online: 07 August 2020

Zheng Li, Vladimir Koval , Amit Mahajan, Zhipeng Gao, Carlo Vecchini, Mark Stewart, Markys G. Cain , Kun Tao, Chenglong Jia , Giuseppe Viola, and Haixue Yan 



View Online



Export Citation



CrossMark

## ARTICLES YOU MAY BE INTERESTED IN

[Intrinsic piezoelectricity in \(K,Na\)NbO<sub>3</sub>-based lead-free single crystal: Piezoelectric anisotropy and its evolution with temperature](#)

Applied Physics Letters **117**, 052904 (2020); <https://doi.org/10.1063/5.0012124>

[Current-induced bulk magnetization of a chiral crystal CrNb<sub>3</sub>S<sub>6</sub>](#)

Applied Physics Letters **117**, 052408 (2020); <https://doi.org/10.1063/5.0017882>

[Magnetic transition behavior and large topological Hall effect in hexagonal Mn<sub>2-x</sub>Fe<sub>1+x</sub>Sn \(x = 0.1\) magnet](#)

Applied Physics Letters **117**, 052407 (2020); <https://doi.org/10.1063/5.0011570>



**Measure Ready**  
**FastHall™ Station**

The highest performance Hall effect system...  
for van der Pauw and Hall bar samples

[Learn more](#)

Lake Shore  
CRYOTRONICS

# Room-temperature multiferroic behavior in layer-structured Aurivillius phase ceramics

Cite as: Appl. Phys. Lett. **117**, 052903 (2020); doi: [10.1063/5.0017781](https://doi.org/10.1063/5.0017781)

Submitted: 9 June 2020 · Accepted: 25 July 2020 ·

Published Online: 7 August 2020 · Corrected: 11 August 2020



View Online



Export Citation



CrossMark

Zheng Li,<sup>1</sup> Vladimir Koval,<sup>2</sup> Amit Mahajan,<sup>3</sup> Zhipeng Gao,<sup>4</sup> Carlo Vecchini,<sup>5</sup> Mark Stewart,<sup>5</sup> Markys G. Cain,<sup>6</sup> Kun Tao,<sup>7</sup> Chenglong Jia,<sup>7,a)</sup> Giuseppe Viola,<sup>3</sup> and Haixue Yan<sup>3,b)</sup> 

## AFFILIATIONS

<sup>1</sup>G... 430074, C  
<sup>2</sup>I... 47, K 04001, ...  
<sup>3</sup>E... E14N, ... K f ...  
<sup>4</sup>N... 621900, C  
<sup>5</sup>N... 110L, ... K ...  
<sup>6</sup>E... G 99, ... K ...  
<sup>7</sup>f... 730000, C

a)Email: ...@... .

b)Author to whom correspondence should be addressed: ...@... .

## ABSTRACT

M... H... A... B<sub>5.25</sub>L<sub>0.75</sub>F<sub>3</sub>O<sub>18</sub>... in situ... F<sup>3+</sup>O<sup>3+</sup>, C<sup>3+</sup>O<sup>3+</sup>, F<sup>3+</sup>O<sup>3+</sup>... C /F...

Published under license by AIP Publishing. [:// . /10.1063/5.0017781](https://doi.org/10.1063/5.0017781)

M<sub>2</sub> (FM)<sub>2</sub> (FE)<sub>2</sub> A B<sub>5</sub>F<sub>3</sub>O<sub>15</sub> (=4)<sup>a</sup> B<sub>6</sub>F<sub>2</sub>O<sub>18</sub> B<sub>4</sub>O<sub>12</sub> B<sub>5</sub>F<sub>0.5</sub>C<sub>0.5</sub>O<sub>15</sub> ( =5) A<sup>14,15</sup> H<sub>a</sub> D<sup>16</sup> B<sub>2</sub>O<sub>3</sub> 7 11 A

$B_{2cb}$   $a = 5.4530(2) \text{ \AA}$ ,  $b = 5.4427(1) \text{ \AA}$ ,  $c = 50.670(2) \text{ \AA}$ ,  $b = 5.3943(6) \text{ \AA}$ ,  $c = 41.487(2) \text{ \AA}$

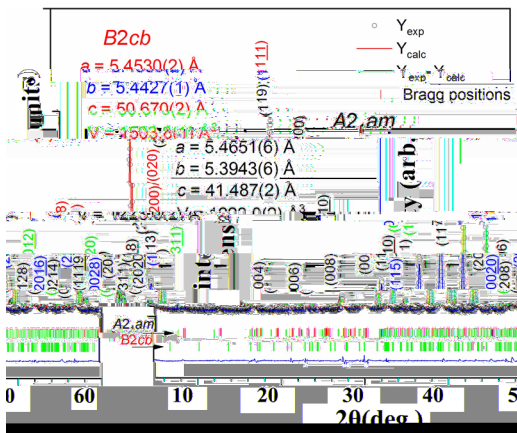


FIG. 1. XRD patterns of B2cb and A2,1am phases.

BLFC  $B_{2cb}$   $a = 5.4530(2) \text{ \AA}$ ,  $b = 5.4427(1) \text{ \AA}$ ,  $c = 50.670(2) \text{ \AA}$ ,  $b = 5.3943(6) \text{ \AA}$ ,  $c = 41.487(2) \text{ \AA}$

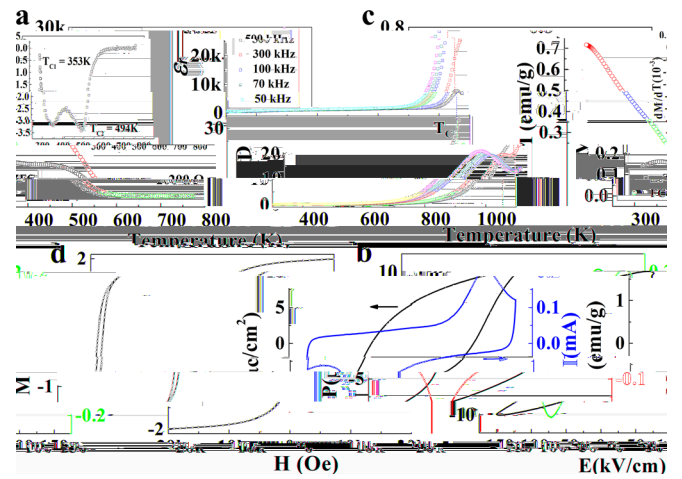


FIG. 2. (a) Temperature dependence of the dielectric constant  $\epsilon'$  and loss  $\epsilon''$  for B2cb at various frequencies. (b) Temperature dependence of the dielectric constant  $\epsilon'$  and loss  $\epsilon''$  for A2,1am at various frequencies. (c) Temperature dependence of the dielectric constant  $\epsilon'$  and loss  $\epsilon''$  for B2cb at various frequencies. (d) Temperature dependence of the dielectric constant  $\epsilon'$  and loss  $\epsilon''$  for A2,1am at various frequencies.

$\sim 494$  K  
 $B_6FC_3O_{18}$  (526 K).<sup>23</sup>  
 BLFC  
 $F^{3+} O F^{3+}, C_a^{3+} O C_a^{3+}, F^{3+} O C^{3+}$  ( $\dots$ ).<sup>24</sup>  
 $ED$   
 $FC$   $\sim 353$  K  
 $C_2F_2O_4$   
 $C_2F_2O_4$  (460 K)  
 $(M)$   $C_2F_2O_4$ <sup>16,25</sup>  
 $16.235$  /  $\dots$ <sup>25</sup>  
 $C_2F_2O_4$   $0.22$   $0.32$  /  $\dots$   
 $M = 1.85$  /  $F_a \cdot 2(\dots)$   $I$  BLFC  
 $M H$   
 $2(F_a \cdot 3)$   
 $425$  K  $1.58$  /  $\dots$   
 $0.27$  /  $\dots$  ED  
 $BLFC$   
 $F_a \cdot 3$   
 $(DF)$   $F^{3+} O C^{3+}$  *ab initio*  
 $(A P)$   
 $F = 2$   $C = 3$   $F_a$   $C_a$   
 $(GGA) + \dots I$   
 $F \cdot 3(\dots)$  BLFC  $F^{3+}$   $C^{3+}$  ( $3.1$   $2.1 \mu_B/a$ )  
 $0.1 \mu_B/a$   $F O_6$   $C O_6$   
 $F/C$   $F \cdot 3(\dots)$   
 $F$   $O$   $F^{3+}$   $C^{3+}$   
 $(\dots)$   $(\dots)$   
 $E_{FM} - E_{AFM}$   
 $= -144.1$   
 $H$   $43.5$  ( $\dots, 504.6$  K), (FM) FM  
 $FC/FC$   $F \cdot 2(\dots)$  *ab*  
 $010$   
 $BLFC$   $F_a \cdot 4$   
 $I$

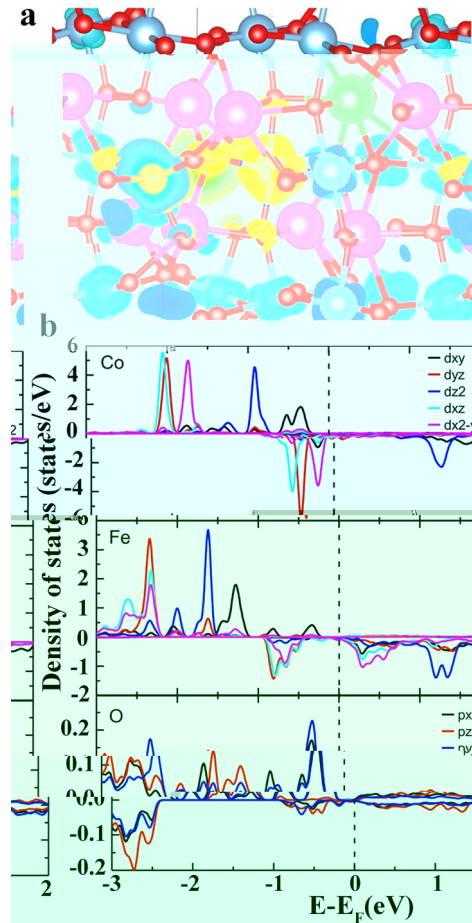


FIG. 3. (a) Crystal structure of BLFC. (b) Density of states (DOS) plots for Co, Fe, and O atoms. The x-axis is  $E - E_f$  (eV) and the y-axis is Density of states (states/eV). The legend indicates the contributions of different orbitals: dxy (black), dyz (red), dz2 (blue), dxz (cyan), dx2-y2 (magenta), px (green), and py (orange).

$N$   
 $(0, 1, 20)$   
 $2 \leq H < 5$   
 $M H$   $F_a \cdot 2(\dots)$   $3 F_a$   
 $F_a \cdot 5$  BLFC P F M  
 $PFM$  BLFC  $399 O$   
 $5(\dots)$  A P

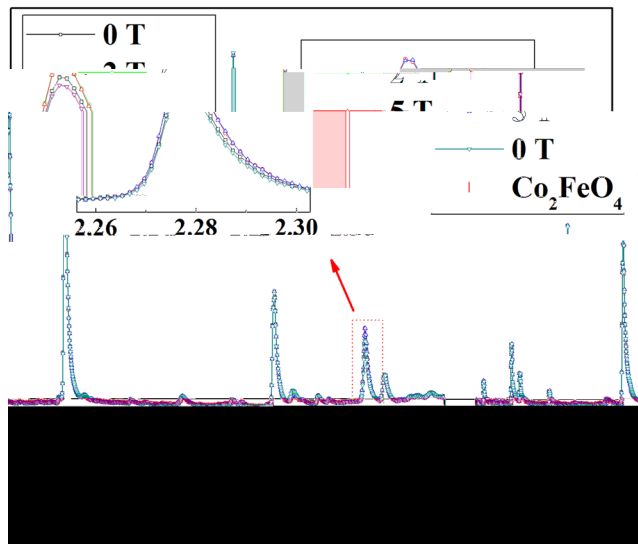


FIG. 4. XRD patterns of  $\text{Co}_2\text{FeO}_4$  at 0 T (blue) and 5 T (red). The inset shows the schematic of the sample and measurement setup.

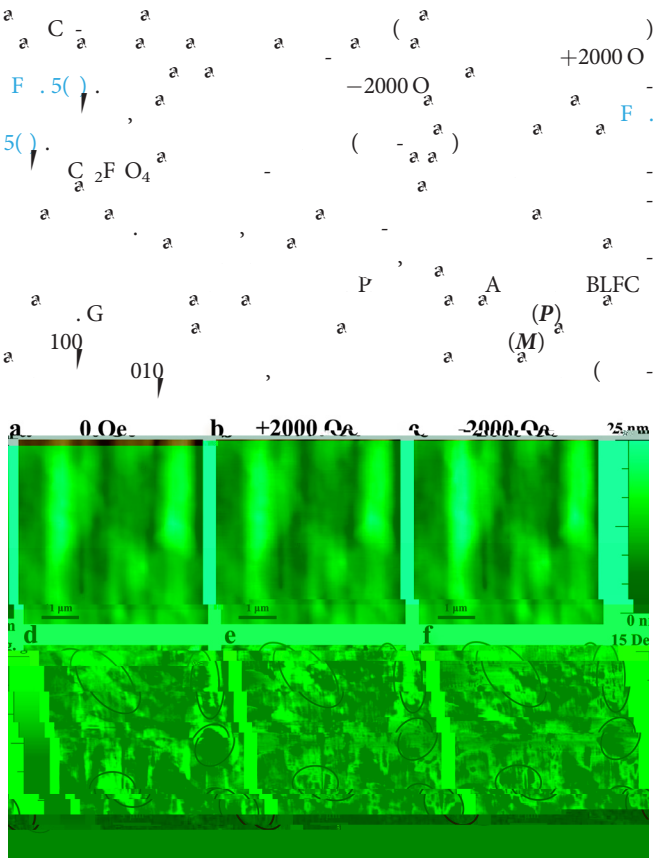


FIG. 5. MFM images of BLFC at different magnetic fields: (a) 0 Oe, (b) +2000 Oe, (c) -2000 Oe. Scale bars are 1 μm and 25 nm.

$T = P \times M$   
 BLFC  
 $\text{C}^{3+} \text{O}_2 \text{C}^{3+} \text{F}^{3+} \text{O}_2 \text{C}^{3+} \text{F}^{3+} \text{O}_2 \text{C}^{3+}$   
 $\text{C}_2\text{F}_2\text{O}_4$   
 EM (ED)  
 BLFC  
 D. M., P., D., K., D.  
 I H I I N, AL,  
 D, O, K.  
 A E D F  
 G A A A A (G N /  
 0038/20), C (G N . K2015-0602006), N FC (G  
 N . 11474138 11834005). A P (EM P)  
 P IND54 N M P (EM P)  
 EM P E AME E

DATA AVAILABILITY

REFERENCES

1. E. A., N. D. M., J. F., N. 442, 759 (2006).
2. N. A., N. M., 6, 21 (2007).
3. J. M., J. H., L., C., N., A. M., 23, 1062 (2011).
4. L. F. H., O. C., J. B., J. L., C. H., H., O. G., D. C. L., H., K., A. J. B., A. F. M., 26, 2111 (2016).
5. N. A. H., J. P. C. B 104, 6694 (2000).
6. B. A., M. : IL.
7. B. A. O<sub>12</sub>, A. K. I(58), 499-512 (1949).
7. A., G. K., M. M. K., J. P. C. M., 11, 3335 (1999).
8. N., P., G., K., M., E., B 108, 194 (2004).
9. L. K., M., M., A. A., N. D., N. P., M., E. P., D. J., J. A. C., 96, 2339 (2013).
10. L., J. M., G., K., A. M., L., C. J., C. N., H., D., 45, 14049 (2016).
11. J. F., NPGA M, 5, 72 (2013).
12. A. B., C. E., P., B 90, 214109 (2014).
13. J. B. L., P. H., G. H., G., L., J. L., J., C., J. K. L., A., P., L., 96, 222903 (2010).
14. M., C., L., A., P., L., 95, 082901 (2009).
15. L., J., L., J. D., A., P., L., 101, 122402 (2012).

- <sup>16</sup>M. P. C., M. B., A. P. B., J. P. H., K., L. K., M. P., C., H. K., A. J. B., *J. A. P.* **112**, 073919 (2012).
- <sup>17</sup>J. L., H., M. J., K., P., *J. A. P.* **102**, 104107 (2007).
- <sup>18</sup>M. G. C., *Characterisation of Ferroelectric Bulk Materials and Thin Films* (2014), 2.
- <sup>19</sup>L., K., J. M., G., K., C. J., G., H., A. M., J. C., M. C., I. A., C. N., C. J., H., *J. M. C. C.* **6**, 2733 (2018).
- <sup>20</sup>K., I., G., M., C. J., H., *J. P. C. C.* **122**, 15733 (2018).
- <sup>21</sup>L. J. F. L., *J. A. C.* **97**, 1 (2014).
- <sup>22</sup>H., F. I., G., H. N., H., J., G., M. J., *J. A. D.* **1**, 107 (2011).
- <sup>23</sup>J., L., L., J. D., A.
- <sup>24</sup>B., J., J. C., L., J. D., A. P. L. **101**, 012402 (2012).
- <sup>25</sup>L. P. M., N. B., *J. P. L.* **104**, 062413 (2014).
- J. P. L.* **11**, 719 (2009).